DOI:10.1190/image2022-3737503.1

3D joint Gramian inversion of airborne gravity gradiometry and magnetotelluric data for geothermal resource exploration

Michael S. Zhdanov, Michael Jorgensen, and Alexander Gribenko, Consortium for Electromagnetic Modeling and Inversion, University of Utah, and TechnoImaging*
Masami Ikeya and Yusuke Usui, Exploration and Production Department, Idemitsu Kosan Co., Ltd.

Summary

Extensive geophysical surveys were conducted over the geothermal field by Japan Oil, Gas and Metals National Corporation (JOGMEC) and Idemitsu Kosan Co. Ltd. (Idemitsu), which included airborne gravity gradiometry (AGG) and magnetotelluric (MT) surveys. The goal of this project was to study the location and structure of geothermal energy sources in the surveys area. The observed AGG and MT data were analyzed separately and jointly using 3D inversion methods. For joint inversion, we used the approach based on Gramian constraints (Zhdanov et al., 2012; Zhdanov, 2015). The Gramian method enforces the correlation between the different physical parameters of the inverse models, or their transforms, thus ensuring that the inversion produces a consistent image of the subsurface geological formation. This paper summarizes the principles of the joint inversion algorithm used in the project. We also present the results of the standalone and joint inversions to demonstrate the effectiveness of the developed method for geothermal resource exploration.

Introduction

JOGMEC collected a total of about 400 line-km of AGG data in the prospective geothermal area of Japan in 2017. Idemitsu also collected a total of 160 stations of MT data in the area of interest (AOI), shown by red dots in Figure 1. Part of MT data was obtained with the support of JOGMEC grant. This geophysical study aimed to determine zones prospective for geothermal resource exploration. One of the practical approaches to studying geothermal fields is based on electromagnetic methods, which provide information about the electrical conductivity distribution in the survey area. For example, several case studies used magnetotelluric data for this purpose (e.g., Wannamaker et al. 2004; Newman et al. 2008). It was demonstrated in a number of publications (e.g., Endo et al., 2018; Mochinaga, et al., 2020) that the most efficient approach to study geothermal fields is based on multiphysics data. These multiphysics data provide mutually complementary information about different physical properties of the source rocks, which helps analyze the geothermal system. The gravity gradiometry data, for example, provide important information on not only density structure but also about the location and orientation of the faults and fractures in the survey area. The knowledge of the fault structure is critical in studying fault-controlled geothermal reservoirs.

Magnetotelluric data contain unique information about the deep conductivity structure, which is an indicator of the geothermal source locations.

This paper presents the results of joint inversion of airborne gravity gradiometry (AGG) and magnetotelluric (MT) data collected in the geothermal field in Japan. We use a joint inversion method based on Gramian constraints. This technique enforces the relationships between different model parameters during the inversion process. We discuss the principles of Gramian inversion and present the results of the practical application of this method to the joint inversion of AGG and MT data in the survey area.

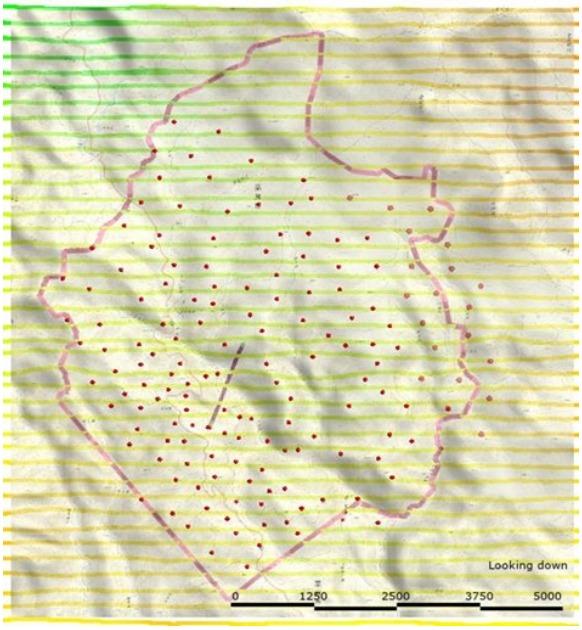

Joint inversion methodology

Gravity gradiometry and MT methods provide information about different physical properties of rock formation, density and conductivity. This information is generally mutually complementary, making it natural to consider a joint inversion of both geophysical datasets. In addition, standalone inversion of the anomalous data response for AGG or MT surveys is subject to considerable uncertainty and ambiguity. One productive approach to reducing

uncertainty is invert AGG and MT data jointly. This additional information can be incorporated in the form of a joint inversion of multiphysics data. This paper uses a novel approach to joint inversion based on Gramian constraints, developed in Zhdanov et al. (2012) and Zhdanov (2015).

Gramian constraints enforce the correlation between different parameters or their transforms. By requiring the minimum of the Gramian mathematical functional in regularized inversion, we obtain multimodal inverse solutions with enhanced correlations between the various model parameters or their attributes.

The gravity and MT inverse problems can be written in the form of the following operator equations:

$$\boldsymbol{d}^{(i)} = A^{(i)}\boldsymbol{m}^{(i)}, (i = 1,2); \quad (1)$$

where $\boldsymbol{d}^{(i)}$ $(i = 1,2)$ are the observed gravity and MT data, and $\boldsymbol{m}^{(i)}$ $(i = 1,2)$ are the unknown density and geoelectrical resistivity distributions, respectively.

Following the principles of Tikhonov regularization and Gramian stabilization (Zhdanov, 2015), we solve equations (1) by minimizing the following joint parametric functional:

$$P^{\alpha}\left(\boldsymbol{m}^{(1)}, \boldsymbol{m}^{(2)}\right) = \sum_{i=1}^{2} \varphi^{(i)}\left(\boldsymbol{m}^{(i)}\right) + \sum_{i=1}^{2} \alpha^{(i)} s_{MN}\left(\boldsymbol{m}^{(i)}\right) + \beta s_G\left(L^{(1)}\boldsymbol{m}^{(1)}, L^{(2)}\boldsymbol{m}^{(2)}\right), \quad (2)$$

where the terms $\varphi^{(i)}$ are the data misfit functionals:

$$\varphi^{(i)}\left(\boldsymbol{m}^{(i)}\right) = \left\| W_d^{(i)}\left(A^{(i)}\left(\boldsymbol{m}^{(i)}\right) - \boldsymbol{d}^{(i)}\right)\right\|^2, (i = 1,2); \quad (3)$$

$W_d^{(i)}$ $(i = 1,2)$ are the data weighting operators; and $A^{(i)}$ $(i = 1,2)$ are the forward modeling operators. The terms $s_{MN}\left(\boldsymbol{m}^{(i)}\right)$ are the minimum norm stabilizing functionals:

$$s_{MN}\left(\boldsymbol{m}^{(i)}\right) = \left\| W_m^{(i)}\left(\boldsymbol{m}^{(i)} - \boldsymbol{m}_{apr}^{(i)}\right)\right\|^2, \quad (4)$$

where $W_m^{(i)}$ $(i = 1,2)$ are the model weighting operators, and $\boldsymbol{m}_{apr}^{(i)}$ $(i = 1,2)$ are the a priori models. The Gramian constraint term for a direct correlation of the model parameters, $s_G\left(L^{(1)}\boldsymbol{m}^{(1)}, L^{(2)}\boldsymbol{m}^{(2)}\right)$, is defined as follows:

$$s_G\left(L^{(1)}\boldsymbol{m}^{(1)}, L^{(2)}\boldsymbol{m}^{(2)}\right) = \begin{vmatrix} \left(L^{(1)}\boldsymbol{m}^{(1)}, L^{(1)}\boldsymbol{m}^{(1)}\right) & \left(L^{(1)}\boldsymbol{m}^{(1)}, L^{(2)}\boldsymbol{m}^{(2)}\right) \\ \left(L^{(2)}\boldsymbol{m}^{(2)}, L^{(1)}\boldsymbol{m}^{(1)}\right) & \left(L^{(2)}\boldsymbol{m}^{(2)}, L^{(2)}\boldsymbol{m}^{(2)}\right) \end{vmatrix}, \quad (5)$$

where $L^{(i)}$ represents a transformation (linear or nonlinear) of the model parameters, and the operation $(*,*)$ denotes the inner product of two vectors in the Gramian space. The nonlinear transformation allows us to map different model grids onto a common grid and allows for nonlinear correlation of model parameters. We can also use the spatial derivatives of the model in the Gramian term, i.e., the gradient, the Laplacian, etc. This may be more appropriate for regions with complex geometry, where petrophysical correlations may not exist. In this structural approach, the Gramian term provides a measure of the correlation between the gradients of model parameters. By imposing an additional requirement minimizing the Gramian in regularized inversion, we obtain multimodal inverse solutions with the enhanced structural similarity between the various model parameters.

The meaning of Gramian and its role in the joint inversion can be better explained using a probabilistic approach to inverse problem solution. In the framework of this approach, one can treat the observed data and the model parameters as the realizations of some random variables. Under this assumption, Gramian can be considered as a determinant of the covariance matrix between different model parameters (Zhdanov et al., 2021):

$$G\left(m^{(1)}, m^{(2)}\right) = \begin{vmatrix} cov\left(m^{(1)}, m^{(1)}\right) & cov\left(m^{(1)}, m^{(2)}\right) \\ cov\left(m^{(2)}, m^{(1)}\right) & cov\left(m^{(2)}, m^{(2)}\right) \end{vmatrix} = \begin{vmatrix} \sigma_1^2 & cov\left(m^{(1)}, m^{(2)}\right) \\ cov\left(m^{(2)}, m^{(1)}\right) & \sigma_2^2 \end{vmatrix} = \sigma_1^2\sigma_2^2\left[1 - \eta^2\left(m^{(1)}, m^{(2)}\right)\right], \quad (6)$$

where $cov\left(m^{(1)}, m^{(2)}\right)$ represents a covariance between two random variables, $m^{(1)}$ and $m^{(2)}$, σ_1 and σ_2 are standard deviations of the random variables corresponding to parameters $m^{(1)}$ and $m^{(2)}$, respectively, and coefficient, η, is a correlation coefficient between these two parameters:

$$\eta\left(m^{(1)}, m^{(2)}\right) = \frac{cov\left(m^{(1)}, m^{(2)}\right)}{\sigma_1^2\sigma_2^2}. \quad (7)$$

The last expression shows that the Gramian provides a measure of the correlation between two parameters, $m^{(1)}$ and $m^{(2)}$. Indeed, the Gramian goes to zero when the correlation coefficient is close to one, corresponding to linear correlation. This property shows that by imposing the Gramian constraint, we enforce a linear correlation between the model parameters.

Note that in the application of the joint Gramian inversion to the AGG and MT data, we have selected parameter $m^{(1)}$ equal to density, ρ, and parameter, $m^{(2)}$, to be equal to the logarithm of conductivity, log σ. Thus, by using the nonlinear transformation (e.g., log σ), one can enforce nonlinear correlations with Gramian stabilizing functional.

3D joint Gramian inversion of airborne gravity gradiometry and magnetotelluric data for geothermal resource exploration

Density and conductivity models produced by joint AGG and MT data inversion

We have performed standalone and joint 3D inversions of AGG and MT using seven components of the GG tensor and vertical gravity component data at 82,143 stations and four components of MT impedance tensor data at 160 stations and 25 frequencies.

Figure 2 shows maps of the observed and predicted AGG and gravity field data for joint inversion as an example. One can see that the agreements between observed and predicted data are reasonably well. The RMS misfit converges to 1.88.

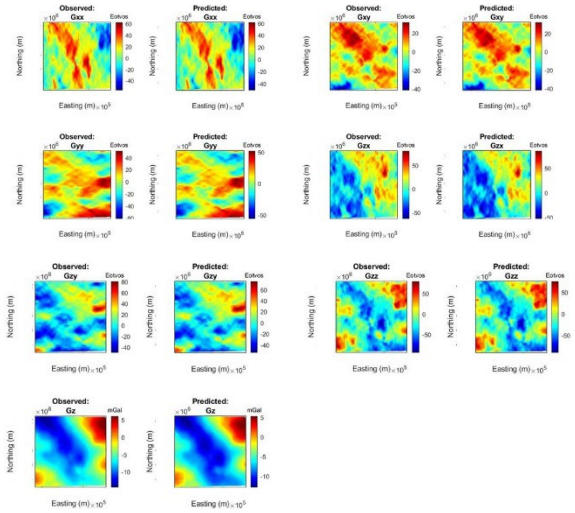

Figure 2: The maps of the observed and predicted gravity gradiometry and gravity data produced by joint Gramian inversion.

Figure 3 shows plots of the observed and predicted MT data for one of MT stations as an example. Figure 4 presents the distribution of the RMS misfit per station. One can see a reasonable agreement between observed and predicted data. The RMS misfit converges to 1.52.

Figure 5 presents a comparison between the density models produced by standalone AGG inversion and a joint inversion with MT data. Figure 6 shows a similar comparison for inverse conductivity models produced by standalone and joint inversions.

The standalone gravity inversion produces a local negative anomalous density structure coinciding with the conductivity anomaly in the central part of the profile (Figure 5, left panel). However, the result of joint inversion (Figure 5, right panel) shows a more detailed image of the anomalous density, which has a similar structure to that of the conductivity anomaly (Figure 6).

At the same time, the conductivity anomaly produced by joint inversion of the AGG and MT data (Figure 6, right panel) has a slightly larger horizontal extension than one produced by standalone MT data inversion (Figure 6, left panel)

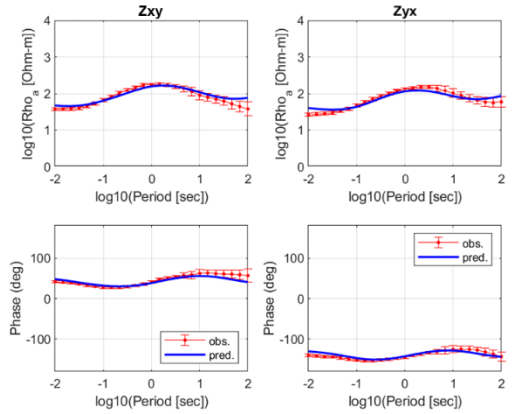

Figure 3: Observed and predicted apparent resistivity (top) and phase (bottom) data for MT station #40. Red dots show the observed data, while blue lines correspond to the predicted data.

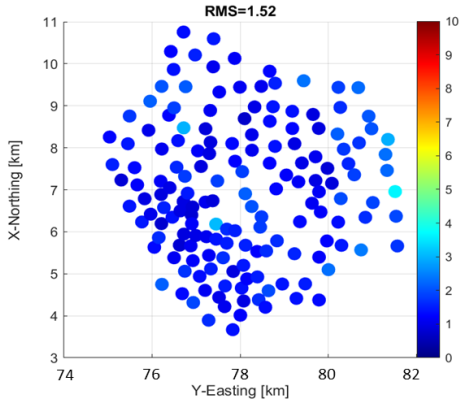

Figure 4: RMS misfit shown for each MT station.

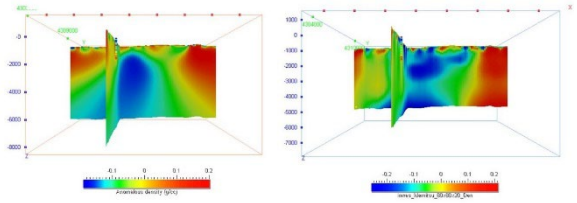

Figure 5: Vertical sections of the 3D density models produced by standalone inversion of the AGG data (left panel) and a joint Gramian inversion (right panel).

3D joint Gramian inversion of airborne gravity gradiometry and magnetotelluric data for geothermal resource exploration

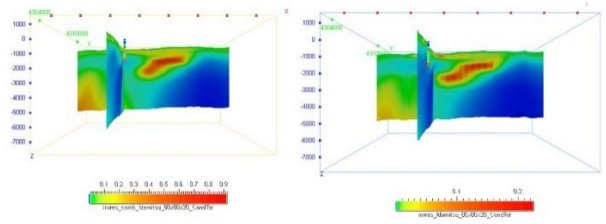

Figure 6: Vertical sections of the 3D conductivity models produced by standalone inversion of the MT data (left panel) and a joint Gramian inversion (right panel).

Comparison of the inversion results with geology

Figures 7 and 8 compare the known schematic geologic section with the jointly inverted density and resistivity models along with profile AA', crossing over the central part of the survey area. The density model correlates well with several different geologic units in the upper part of the geologic section, indicating the presence of faults (Figure 7). This information is critical for understanding the structure of fault-controlled geothermal reservoirs.

The geoelectric model shows the potential location of a geothermal source in the north-eastern part of the survey area, which is manifested by the low resistivity anomaly in that area shown by red color in Figure 8.

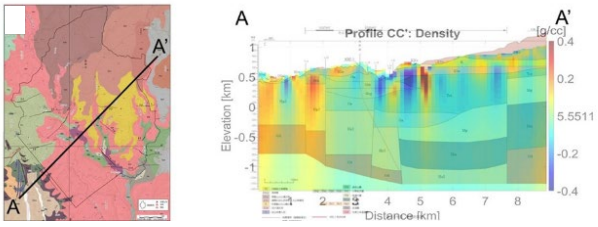

Figure 7: Profile AA' location (left panel). The joint inversion density model is superimposed over the geologic section along AA' (right panel).

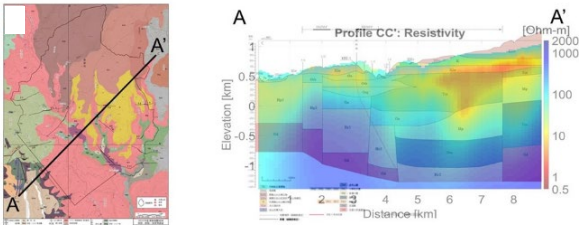

Figure 8: Profile AA' location (left panel). The joint inversion resistivity model is superimposed over the geologic section along AA" (right panel).

Conclusions

We have developed and applied the joint inversion of multiphysics data to interpret AGG and MT data collected over a known geothermal field in Japan. The method is based on Gramian constraint to stimulate the mutual dependence between the anomalous density and conductivity of the same rock formations under investigation. The Gramian inversion produced consistent density and conductivity models of the subsurface geology in the study area. In the joint inversion, both density and resistivity images were improved. Furthermore, this joint inversion approach makes it possible to determine regions representing fractured geothermal reservoirs, based on the inverse density model, and simultaneously find the low resistive zones of geothermal source locations.

Therefore, joint inversion of multiphysics data has the potential to increase the success rate of drilling, thus reducing the cost of geothermal resource exploration.

Acknowledgments

The authors acknowledge TechnoImaging, the Consortium for Electromagnetic Modeling and Inversion (CEMI) of The University of Utah, Idemitsu Kosan Co., Ltd. and Japan Oil, Gas and Metals National Corporation (JOGMEC) for the support of this project and permission to publish.

REFERENCES

Cox, L. H., and M. S. Zhdanov, 2007, Large-scale 3D inversion of HEM data using a moving footprint: 77th Annual International Meeting, SEG, Expanded Abstracts, 467–471, doi: https://doi.org/10.1190/1.2792464.

Endo, M., A. Gribenko, D. Sunwall, M. S. Zhdanov, T. Miura, H. Mochinaga, N. Aoki, and T. Mouri, 2018, Integrated interpretation of multimodal geophysical data for exploration of geothermal resources — Case study: Yamagawa geothermal field in Japan: 88th Annual International Meeting, SEG, Expanded Abstracts, 1949–4645, doi: https://doi.org/10.1190/segam2018-2997562.1.

Gribenko, A. V., and M. S. Zhdanov, 2017, 3-D inversion of the MT EarthScope data, collected over the east central United States: Geophysical Research Letters, **44**, 800–807, doi: https://doi.org/10.1002/2017GL075000.

Li, X., and M. Chouteau, 1998, Three-dimensional gravity modeling in all space: Surveys in Geophysics, **19**, 339–368, doi: https://doi.org/10.1023/A:1006554408567.

Li, Y., and D. W. Oldenburg, 1996, 3-D inversion of magnetic data: Geophysics, **61**, 394–408, doi: https://doi.org/10.1190/1.1443968.

Li, Y., and D. W. Oldenburg, 1998, 3-D inversion of gravity data: Geophysics, **63**, 109–119, doi: https://doi.org/10.1190/1.1444302.

Mochinaga, H., N. Aoki, D. Sunwall, M. Zhdanov, and T. Mouri, 2020, Probabilistic approach for 3D conceptual modeling using multi geophysical data: Proceedings World Geothermal Congress.

Newman, G. A., E. Gasperikova, G. M. Hoversten, and P. E. Wannamaker, 2008, Three-dimensional magnetotelluric characterization of the Coso geothermal field: Geothermics, **37**, 369–399, doi: https://doi.org/10.1016/j.geothermics.2008.02.006.

Okabe, M., 1979, Analytical expressions for gravity anomalies due to homogeneous polyhedral bodies and translations into magnetic anomalies: Geophysics, **44**, 730–741, doi: https://doi.org/10.1190/1.1440973.

Pilkington, M., 1997, 3-D magnetic imaging using conjugate gradients: Geophysics, **62**, 1132–1142, doi: https://doi.org/10.1190/1.1444214.

Portniaguine, O., and M. S. Zhdanov, 1999, Focusing geophysical inversion images: Geophysics, **64**, 874–887, doi: https://doi.org/10.1190/1.1444596.

Wannamaker, P. E., P. E. Rose, W. M. Doerner, B. C. Berard, J. McCulloch, and K. Nurse, 2004, Magnetotelluric surveying and monitoring at the Coso geothermal area, California, in support of the enhanced geothermal systems concept: Survey parameters and initial results: Proceedings of the 29th Workshop on Geothermal Reservoir Engineering, Stanford University.

Zhdanov, M. S., 2002, Geophysical inverse theory and regularization problems: Elsevier.

Zhdanov, M. S., 2009, New advances in regularized inversion of gravity and electromagnetic data: Geophysical Prospecting, **57**, 463–478, doi: https://doi.org/10.1111/j.1365-2478.2008.00763.x.

Zhdanov, M. S., 2015, Inverse theory and applications in geophysics: Elsevier.

Zhdanov, M. S., 2018, Foundations of geophysical electromagnetic theory and methods: Elsevier.

Zhdanov, M. S., A. Green, A. Gribenko, and M. Čuma, 2010, Large-scale three-dimensional inversion of EarthScope MT data using the integral equation method: Physics of the Earth, **8**, 27–35.

Zhdanov, M. S., M. Jorgensen, and L. Cox, 2021, Advanced methods of joint inversion of multiphysics data for mineral exploration: Geosciences, **11**, 262, doi: https://doi.org/10.3390/geosciences11060262.